J|A|C|S ARTICLES

Published on Web 03/31/2009

Influence of Charge State on Catalytic Oxidation Reactions at Metal Oxide Clusters Containing Radical Oxygen Centers

Grant E. Johnson,[†] Roland Mitrić,[‡] Melanie Nössler,[‡] Eric C. Tyo,[†] Vlasta Bonačić-Koutecký,[‡] and A. W. Castleman, Jr.*,[†]

Departments of Chemistry and Physics, The Pennsylvania State University, University Park, Pennsylvania 16802, and Institut für Chemie, Humboldt-Universität zu Berlin, Brook-Taylor-Strasse 2, 12489 Berlin, Germany

Received September 21, 2008; E-mail: awc@psu.edu

Abstract: Evidence obtained by guided-ion-beam mass spectrometry experiments and density functional theory calculations indicates that by adding one oxygen atom with a full octet of valence electrons (O^{2-}) to stoichiometric cationic zirconium oxide clusters $(ZrO_2)_x^+$ ($x = 1-4$), a series of anionic clusters $(Zr_xO_{2x+1})^-$ ($x = 1-4$) are formed which contain radical oxygen centers with elongated (elongation $\approx 0.24 \pm 0.02$ Å) metal−oxygen bonds. These anionic clusters oxidize carbon monoxide, strongly associate acetylene, and weakly associate ethylene, in contrast to the cationic species which were found previously to be highly active toward the oxidation of all three molecules. Theoretical investigations indicate that a critical hydrogen transfer step necessary for the oxidation of ethylene and acetylene at metal oxide clusters containing radical oxygen centers is energetically favorable for cationic clusters but unfavorable for the corresponding anionic species. The calculated electrostatic potential of the cluster reveals that in the case of cations, a favorable interaction with nucleophilic molecules takes place over the whole surface of the $(ZrO_2)_x^+$ ($x = 1-4$) clusters, compared to a restricted interaction of ethylene and acetylene with the less coordinated zirconium atom in the case of the anionic $(Zr_xO_{2x+1})^-$ ($x = 1-4$) species. Therefore, in spite of the common presence of a radical oxygen center in specific anionic and cationic stoichiometries, the extent to which various classes of reactions are promoted is influenced by charge state. Moreover, the $(Zr_xO_{2x+1})^-$ ($x = 1-4$) series of anionic clusters may be regenerated by reacting oxygen deficient clusters with a strong oxidizer. This indicates that not only cationic species, as shown previously, but also anionic clusters may promote multiple cycles of carbon monoxide oxidation.

Introduction

Studies of gas-phase clusters have revealed that species with particular sizes and stoichiometries often exhibit greatly enhanced activity toward specific reactions.[1,2] Of primary interest to heterogeneous oxidation catalysis is the reactive behavior of transition metal and main group metal oxides which are widely used in industry as catalyst and catalyst−support materials.[3−5] Previous studies in our laboratories,[6−8] and by others[9−12] have shown that stoichiometric cationic metal oxide clusters containing radical oxygen (M-O•) centers with elongated metal−oxygen bonds are active toward the selective oxidation of carbon monoxide (CO) and unsaturated hydrocarbons as well as the activation of the carbon−hydrogen bonds of saturated hydrocarbons. Furthermore, several experiments have indicated the presence of radical oxygen species in bulk-phase vanadia and molybdena catalysts used in the selective oxidation of methane,[13] ethane[14] and benzene,[15,16] emphasizing the importance of gas-phase cluster findings for basic understanding of the catalytic mechanisms involved in practical industrial and commercial applications.

In a recent publication[6] we provided evidence that a series of stoichiometric cationic zirconium oxide clusters

[†] The Pennsylvania State University.
[‡] Humboldt Universität zu Berlin.

(1) Zemski, K. A.; Justes, D. R.; Castleman, A. W., Jr. *J. Phys. Chem. B* **2002**, *106*, 6136–6148.
(2) Böhme, D. K.; Schwarz, H. *Angew. Chem., Int. Ed.* **2005**, *44*, 2336–2354.
(3) Thomas, J. M.; Thomas, W. J. *Principals and Practice of Heterogeneous Catalysis*; VCH: New York, 1996.
(4) Anderson, J. A.; Garcia, M. F. *Supported Metals in Catalysis*; Imperial College Press: London, 2005.
(5) Somorjai, G. A. *Introduction to Surface Chemistry and Catalysis*; John Wiley & Sons: New York, 1994.
(6) Johnson, G. E.; Mitrić, R.; Tyo, E. C.; Bonačić-Koutecký, V.; Castleman, A. W., Jr. *J. Am. Chem. Soc.* **2008**, *130*, 13912–13920.
(7) Justes, D. R.; Mitrić, R.; Moore, N. A.; Bonačić-Koutecký, V.; Castleman, A. W., Jr. *J. Am. Chem. Soc.* **2003**, *125*, 6289–6299.
(8) Moore, N. A.; Mitrić, R.; Justes, D. R.; Bonačić-Koutecký, V.; Castleman, A. W., Jr. *J. Phys. Chem. B* **2006**, *110*, 3015–3022.
(9) Feyel, S.; Schröder, D.; Schwarz, H. *J. Phys. Chem. A* **2006**, *110*, 2647–2654.
(10) Feyel, S.; Döbler, J.; Schröder, D.; Sauer, J.; Schwarz, H. *Angew. Chem., Int. Ed.* **2006**, *45*, 4681–4685.
(11) Feyel, S.; Döbler, J.; Hokendorf, R.; Beyer, M. K; Sauer, J.; Schwarz, H. *Angew. Chem., Int. Ed.* **2008**, *47*, 1946–1950.
(12) Schröder, D.; Roithova, J. *Angew. Chem., Int. Ed.* **2006**, *45*, 5705–5708.
(13) Liu, H. F.; Liu, R. S.; Liew, K. Y.; Johnson, R. E.; Lunsford, R. H. *J. Am. Chem. Soc.* **1984**, *106*, 4117–4121.
(14) Yang, T. S.; Lunsford, J. H. *J. Catal.* **1980**, *63*, 505–509.
(15) Iwamoto, M.; Hirata, I.; Matsukami, K.; Kagawa, S. *J. Phys. Chem.* **1983**, *87*, 903–905.
(16) Panov, G. I.; Dubkov, K. A.; Starokon, E. V. *Catal. Today.* **2006**, *117*, 148–155.

10.1021/ja807499z CCC: $40.75

$(ZrO_2)_x^+$ ($x = 1-4$) containing radical oxygen centers are particularly reactive toward the selective oxidation of CO, ethylene (C_2H_4), and acetylene (C_2H_2). Through a combination of experiments in the gas-phase and density functional theory calculations we determined that each reaction is highly favorable energetically and involves easily surmountable barriers. Furthermore, we found that the active stoichiometric clusters may be regenerated by reacting oxygen deficient cationic zirconium oxides with nitrous oxide (N_2O), thereby completing a full catalytic cycle. These findings led us to conclude that the stoichiometric series of cationic zirconium oxide clusters are potential building blocks for a cluster assembled catalyst that would efficiently promote three oxidation reactions of widespread chemical relevance.[6]

In addition to identifying the active centers that promote reactions, understanding how charging effects influence catalytic processes is relevant to the directed design of future catalysts. Charge transfer interactions between catalyst particles and support materials have been shown to exert a pronounced influence on catalytic activity.[17] Indeed, charge transfer to small gold clusters trapped at oxygen vacancies on magnesium oxide surfaces has been shown to be crucial to CO oxidation activity.[18,19] In addition, recent work[20−22] has found that charging of adsorbed metals does not always involve the presence of defects on the oxide surface. Both experimental and theoretical studies have verified the presence of charged gold species on thin defect-free MgO surfaces supported on Mo and Ag.[20−22] It is proposed that by varying the thickness of the MgO layer, and thereby the work function of the underlying metal, it may be possible to tune the charging of the supported Au clusters.[21] Transfer of electrons through thin alumina films into supported gold chains has also been observed.[23] These previous findings emphasize the importance of charge transfer interactions in materials that are used as heterogeneous catalysts.

Gas-phase clusters, which may be studied experimentally and theoretically in a well defined charge state as either a cation or an anion, serve as tractable model catalytic systems that are uniquely capable of providing evidence for the effect of charge state at active sites that promote catalytic oxidation reactions. Furthermore, in several instances, full catalytic cycles have been observed in the gas phase, thereby providing insight into the elementary mechanisms of catalytic reactions.[24−31] For example, in a recent publication we described how the charge state of small gold oxide clusters directly influences the mechanism of CO oxidation.[32] On the basis of these previous findings, fundamental questions can be raised as to whether the presence of oxygen radical centers in metal oxide clusters is alone sufficient to promote the oxidation of CO and unsaturated hydrocarbons, or whether an interplay between oxygen radical sites and a specific charge state is necessary to enable reactivity.

Herein, we present results from our joint experimental and theoretical investigation of the influence of differing charge states on the oxidation of CO, C_2H_2 and C_2H_4 at zirconium oxide clusters containing radical oxygen centers. Our findings, obtained by guided-ion-beam mass spectrometry experiments and density functional theory calculations, indicate that by adding one oxygen atom with a full octet of valence electrons (O^{2-}) to stoichiometric cationic zirconium oxide clusters $(ZrO_2)_x^+$ ($x = 1-4$), a series of anionic clusters are formed $(Zr_xO_{2x+1})^-$ ($x = 1-4$) which contain radical oxygen centers with elongated (elongation $\approx 0.24 \pm 0.02$ Å) metal−oxygen bonds. In contrast to the stoichiometric cationic zirconium oxide clusters studied previously, the anionic clusters oxidize CO to CO_2, strongly associate C_2H_2 and weakly associate C_2H_4. Calculations indicate that the oxidation of CO is favorable with easily surmountable energy barriers. However, a critical hydrogen transfer step required for the oxidation of C_2H_2 and C_2H_4, which is favorable for the cationic clusters, is calculated to involve a barrier that is higher in energy than the reactants making the oxidation of these molecules unfavorable at anionic clusters. Moreover, the electrostatic potential of the $(ZrO_2)_x^+$ and $(Zr_xO_{2x+1})^-$ ($x = 1-4$) clusters is calculated to change dramatically between different charge states and directly influences the extent to which various classes of reactions are promoted. In addition, the anionic series of clusters containing radical oxygen centers may be regenerated by reacting oxygen deficient anionic zirconium oxides with N_2O. The presence of a radical oxygen center alone, therefore, is sufficient to promote the catalytic oxidation of CO. Moreover, a combination of a radical oxygen center and positive charge results in a low enough barrier to the critical hydrogen transfer step necessary for the oxidation of C_2H_2 and C_2H_4 by zirconium oxide clusters to occur.

Experimental Methods

The reactivity of anionic zirconium oxide clusters with CO, C_2H_2, C_2H_4 or N_2O was studied using a guided-ion-beam (GIB) mass spectrometer described in detail in a previous publication.[33] Briefly, zirconium oxide clusters were produced in a laser vaporization (LaVa) cluster source by pulsing oxygen seeded in helium (10%) into the plasma formed by ablating a zirconium rod with the second harmonic (532 nm) of a Nd:YAG laser. To prevent the undesired formation of hydroxo species ultrahigh purity helium and oxygen were used to create the expansion gas mixture. Furthermore, all of the gas transfer lines, which are constructed of stainless steel, were heated while under vacuum to desorb any residual water. The clusters exit the source region and are cooled through supersonic expansion into vacuum. During supersonic expansion the high pressure (13.2 atm) expansion gas mixture passes through a narrow diameter nozzle into vacuum. The random thermal energy of the clusters is thereby converted into directed kinetic energy of the

(17) van Santen, R. A.; Neurock, M. *Molecular Heterogeneous Catalysis*; Wiley-VCH: Weinheim, 2006.
(18) Sanchez, A.; Abbet, S.; Heiz, U.; Schneider, W. D.; Häkkinen, H.; Barnett, R. N.; Landman, U. *J. Phys. Chem. A* **1999**, *103*, 9573–9578.
(19) Yoon, B.; Häkkinen, H.; Landman, U.; Wörz, A. S.; Antonietti, J. M.; Abbet, S.; Judai, K.; Heiz, U. *Science* **2005**, *307*, 403–407.
(20) Zhang, C.; Yoon, B.; Landman, U. *J. Am. Chem. Soc.* **2007**, *129*, 2228–2229.
(21) Sterrer, M.; Risse, T.; Pozzoni, U.; Giordano, L.; Heyde, M.; Rust, H.; Pacchioni, G.; Freund, H. *Phys. Rev. Lett.* **2007**, *98*, 096107.
(22) Honkala, K.; Häkkinen, H. *J. Phys. Chem. C* **2007**, *111*, 4319–4327.
(23) Nilius, N.; Ganduglia-Pirovano, M. V.; Brazdova, V.; Kulawik, M.; Sauer, J.; Freund, H. J. *Phys. Rev. Lett.* **2008**, *100*, 09608.
(24) Kappes, M. M.; Staley, R. H. *J. Am. Chem. Soc.* **1981**, *103*, 1286–1287.
(25) Andersson, M.; Rosen, A. *J. Chem. Phys.* **2002**, *117*, 7051–7054.
(26) Schnabel, P.; Weil, K. G.; Irion, M. P. *Angew. Chem., Int. Ed.* **1992**, *31*, 636–638.
(27) Socaciu, L. D.; Hagen, J.; Bernhardt, T. M.; Wöste, L.; Heiz, U.; Häkkinen, H.; Landman, U. *J. Am. Chem. Soc.* **2003**, *125*, 10437–10445.
(28) Bronstrup, M.; Schröder, D.; Kretzschmar, I.; Schwarz, H.; Harvey, J. N. *J. Am. Chem. Soc.* **2001**, *123*, 142–147.
(29) Shi, Y.; Ervin, K. M. *J. Chem. Phys.* **1998**, *108*, 1757–1760.
(30) Balaj, O. P.; Balteanu, I.; Roβteuscher, T. T. J.; Beyer, M. K.; Bondybey, V. E. *Angew. Chem., Int. Ed.* **2004**, *43*, 6519–6522.
(31) Siu, C.-K.; Reitmeier, S. J.; Balteanu, I.; Bondybey, V. E.; Beyer, M. K. *Eur. Phys. J. D* **2007**, *43*, 189–192.
(32) Bürgel, C.; Reilly, N. M.; Johnson, G. E.; Mitrić, R.; Kimble, M. L.; Castleman, A. W., Jr.; Bonačić-Koutecký, V. *J. Am. Chem. Soc.* **2008**, *130*, 1694–1698.
(33) Bell, R. C.; Zemski, K. A.; Justes, D. R.; Castleman, A. W., Jr. *J. Chem. Phys.* **2001**, *114*, 798–811.

molecular beam. Consequently, the internal vibrational and rotational energy of the clusters is lowered through collisions with the He carrier gas. The working pressure in the field free region of the source is between 5 to 9 $\times$ 10^{-5} Torr depending on the length of time that the pulse valve is open per pulse.[33] The kinetic energy imparted to the cluster ions by the supersonic expansion was determined previously, employing a retarding potential analysis,[33] to be approximately 1 eV in the laboratory energy frame ($E_{\mathrm{LABORATORY}}$). Ideally, all clusters exiting the supersonic expansion source have the same initial kinetic energy. The initial center-of-mass collision energy (E_{CM}) was calculated for ZrO_3^-, $Zr_2O_5^-$, $Zr_3O_7^-$, and $Zr_4O_9^-$ to be approximately 0.17, 0.10, 0.07 and 0.05 eV for all three reactant gases (CO, C_2H_2 and C_2H_4). As subsequent collisions are expected to dissipate the initial energy of a given cluster, the values reported above serve to establish an upper limit on the kinetic energy of the reactive collisions.

After exiting the source region the clusters pass through a 3 mm skimmer forming a collimated molecular beam and are then directed into a quadrupole mass filter employing a set of electrostatic lenses. The quadrupole mass filter isolates clusters of a desired mass to charge ratio which are then passed into an octopole collision cell. To maximize the intensity of a mass-selected cluster the resolution of the first quadrupole mass filter was adjusted to discriminate completely between adjacent zirconium oxides in the cluster distribution. Therefore, although care was taken to prevent the formation of zirconium hydroxides in the laser vaporization source, as mentioned above, we cannot exclude that a small percentage of the mass selected ions may consist of these species. Variable pressures of CO, C_2H_2, C_2H_4 or N_2O are introduced into the octopole collision cell employing a low flow leak valve. The gas pressure is monitored using a MKS Baratron capacitance manometer. During reactivity experiments the source region was grounded as was the electrostatic lens at the entrance to the octopole collision cell and the octopole rods, thereby ensuring that no additional kinetic energy was imparted to the cluster ions in excess of that resulting from the supersonic expansion ($E_{\mathrm{LABORATORY}} \approx 1$ eV). Product ions formed in the collision cell are mass analyzed by a second quadrupole mass spectrometer. Again, to maximize the intensity of the product ions the resolution of the second quadrupole mass spectrometer was adjusted to discriminate completely between the formation of various possible oxygen transfer products, which are the focus of this publication. Due to the isotope distribution of zirconium, and the resolution settings employed, we did not experimentally identify any hydrogen abstraction products. Finally, the ions are detected with a channeltron electron multiplier connected to a mutichannel scalar card. The experimental branching ratios presented in the results section and Supporting Information illustrate the change in normalized ion intensity with increasing pressures of reactant gas. At higher gas pressures, therefore, the ratio of reactant ion intensity to total ion intensity becomes smaller while the ratio of product ion intensity to total ion intensity becomes larger. We present the experimental data as pressure dependent normalized ion intensities for the primary reaction channels because the absolute intensities of different mass selected reactant ions vary substantially between species. Product mass spectra at a specific reactant gas pressure would indicate the absolute intensity of both reactant and product ions for a given reaction but would not allow for a comparison of the relative reactivity of different cluster ions. Separate experiments were also conducted with an inert collision partner (Xe) to verify that the products observed with CO, C_2H_4, C_2H_2 or N_2O are the result of a chemical reaction and not the products of collisional fragmentation.

Theoretical Calculations

The structural properties of the anionic $(Zr_xO_{2x+1})^-$ ($x = 1-4$) clusters and their reactivity towards CO, C_2H_2, C_2H_4 or N_2O were studied using the DFT method with the hybrid B3LYP functional.[34−36] For the zirconium atoms a triple-ζ-valence-plus-polarization (TZVP) atomic basis set combined with the Stuttgart group 12-electron relativistic effective core potential (12e-RECP) was employed.[37,38] For the carbon, oxygen and hydrogen atoms the TZVP basis sets were used. Our previous studies of the reactivity of transition metal oxides have shown that such a combination of hybrid density functionals with triple-ζ quality basis sets allow the accurate prediction of the reaction energetics and mechanisms. Comparison of the ground-state properties of transition metal oxide clusters obtained from B3LYP calculations with experimental results of infrared multiphoton dissociation spectroscopy (IRMPD) are in excellent agreement as shown previously, thus confirming that the structural properties are adequately described by the B3LYP approach.[39−41] The error bars for the heat of formation calculated within the B3LYP method were estimated to be about 0.15 eV.[42] For a comparison of the performance of different functionals for transition metals and their oxides, compare refs 43−45. All structures presented were fully optimized using gradient minimization techniques and stationary points were characterized as minima or transition states by calculating the frequencies. Moreover, the reaction mechanisms were determined by calculating the energy profiles based on electronic energies of the DFT calculations. This is justified since the GIB experiments were performed under microcanonical conditions at relatively low pressures. The stationary points on which the reaction mechanisms are based were characterized as minima or transition states by calculating the frequencies. The proposed reaction mechanisms were also confirmed by performing ab initio molecular dynamics (MD) simulations "on the fly" based on the DFT method. Newton's equations of motion are solved using the Verlet algorithm with time steps of 0.5 fs and the forces are calculated employing the analytical energy gradients in the framework of the TURBOMOLE program.[46] The MD simulations performed at constant energy allow the rearrangements of bonds along the reaction pathways to be followed. In order to improve efficiency the resolution of identity (RI)-DFT procedure[47,48] was employed involving the Perdew-Burke-Ernzerhof (PBE)[49] functional.[37] In order to verify the accuracy of functionals the structural properties as well as energy profiles were also calculated using

(34) Becke, A. D. *Phys. Rev. A* **1988**, *38*, 3098–3100.
(35) Becke, A. D. *J. Chem. Phys.* **1993**, *98*, 5648–5652.
(36) Lee, C.; Yang, W.; Parr, R. G. *Phys. Rev. B* **1998**, *37*, 785–789.
(37) Andrea, D.; Haeussermann, U.; Dolg, M.; Stoll, H.; Preuss, H. *Theor. Chim. Acta* **1990**, *77*, 123–141.
(38) Gilb, S.; Weis, P.; Furche, F.; Aldrichs, R.; Kappes, M. M. *J. Chem. Phys.* **2002**, *116*, 4094–4101.
(39) Fielicke, A.; Mitrić, R.; Meijer, G.; Bonačić-Koutecký, V.; von Helden, G. *J. Am. Chem. Soc.* **2003**, *125*, 15716–15717.
(40) Asmis, K. R.; Meijer, G.; Brümmer, M.; Kaposta, C.; Santambrogio, G.; Wöste, L.; Sauer, J. *J. Chem. Phys.* **2004**, *120*, 6461–6470.
(41) Feyel, S.; Schwarz, H.; Schröder, D.; Daniel, C.; Hartl, H.; Döbler, J.; Sauer, J.; Santambrogio, G.; Wöste, L.; Asmis, K. R. *ChemPhysChem* **2007**, *8*, 1640–1647.
(42) Curtiss, L. A.; Raghavachari, K.; Redfern, P. C.; Pople, J. A. *J. Chem. Phys.* **1997**, *106*, 1063–1079.
(43) Furche, F.; Perdew, J. P. *J. Chem. Phys.* **2006**, *124*, 044103.
(44) Zhao, Y; Truhlar, D. G. *J. Chem. Phys.* **2006**, *124*, 224105.
(45) Xu, X.; Faglioni, F.; Goddard, W. A. *J. Phys. Chem. A* **2002**, *106*, 7171–7176.
(46) Ahlrichs, R.; Bär, M.; Häser, M.; Horn, H.; Kölmel, C. *Chem. Phys. Lett.* **1989**, *162*, 165–169.
(47) Dunlap, B. I.; Connolly, J. W. D.; Sabin, J. R. *J. Chem. Phys.* **1979**, *71*, 3396–3402.
(48) Eichkorn, K.; Treutler, O.; Öhm, H.; Häser, M.; Aldrichs, R. *Chem. Phys. Lett.* **1995**, *242*, 652–660.
(49) Perdew, J. P.; Burke, K.; Ernzerhof, M. *Phys. Rev. Lett.* **1996**, *77*, 3865–3868.

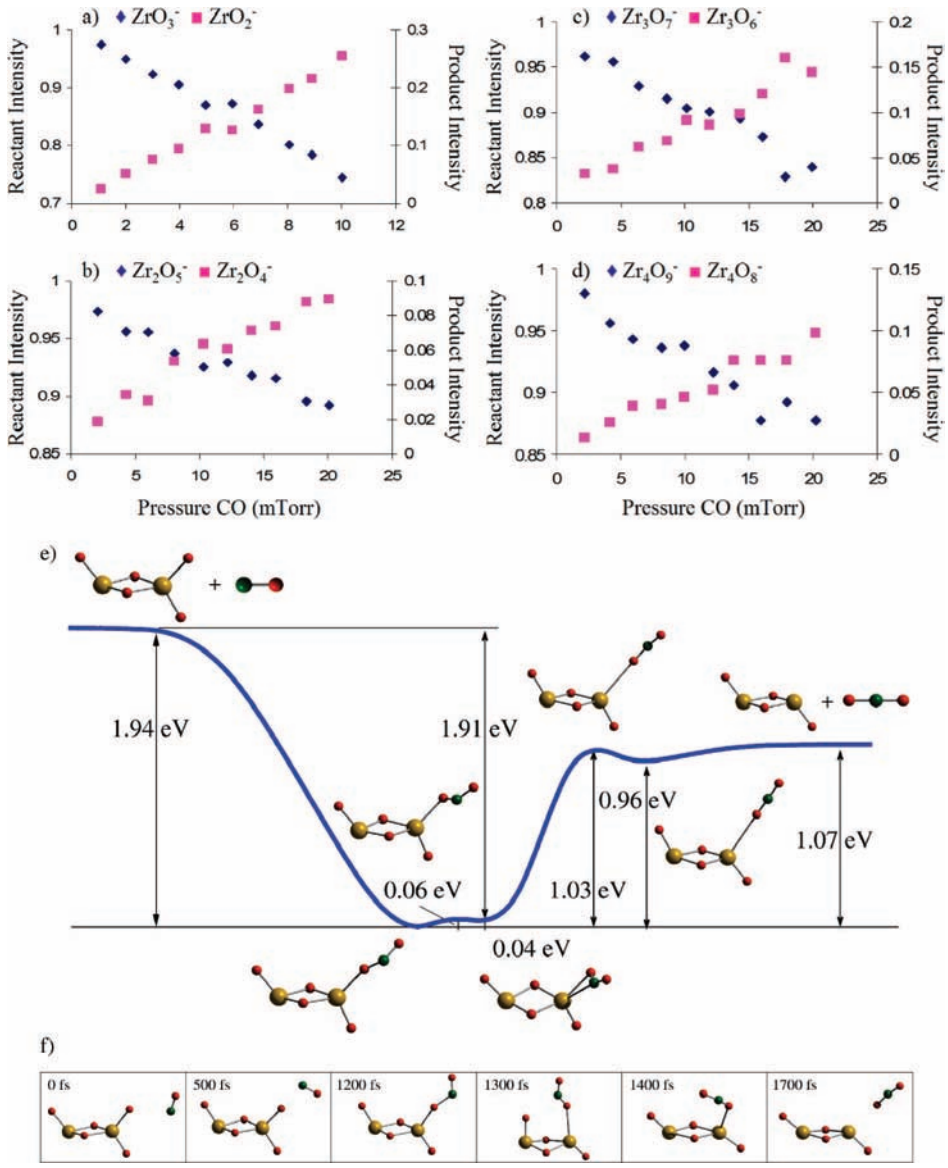

Figure 1. Normalized ion intensities of (a) ZrO_3^-, (b) $Zr_2O_5^-$, (c) $Zr_3O_7^-$ and (d) $Zr_4O_9^-$ with increasing pressure of CO. (e) Calculated energy profile for the reaction of $Zr_2O_5^-$ with CO. (f) Snapshots from MD simulations of the reaction of $Zr_2O_5^-$ with CO.

the PBE functional. Comparison of the results obtained using both functionals (B3LYP and PBE) are provided in the Supporting Information. The most stable structures remain the same. The PBE functional gives rise to slightly lower barriers but the qualitative features of the energy profiles remain unchanged. Therefore discussion of the results throughout the paper will be based on the results obtained using the B3LYP functional.

Results and Discussion

Anionic zirconium oxide clusters containing between one and four zirconium atoms and two to ten oxygen atoms were mass selected and reacted individually with CO, C_2H_2, C_2H_4, or N_2O. Anionic clusters with a $Zr_xO_{2x+1}^-$ ($x = 1-4$) stoichiometry were found to exhibit intense oxygen transfer products consistent with the oxidation of CO to CO_2 according to equation 1.

$$Zr_xO_{2x+1}^- (x = 1-4) + CO \rightarrow Zr_xO_{2x}^- + CO_2 \qquad (1)$$

Minor products resulting from the exothermic degradation of the clusters into smaller zirconium oxide units were also observed but are not included in Figure 1 because of their negligible intensity compared to the dominant oxygen transfer product. The normalized ion intensities of ZrO_3^-, $Zr_2O_5^-$, $Zr_3O_7^-$ and $Zr_4O_9^-$ with increasing pressure of CO reactant gas are displayed in Figures 1a−d, respectively. The experimental results reveal a decrease in the normalized intensity of each of the reactant ions $(Zr_xO_{2x+1})^-$ ($x = 1-4$) accompanied by a pronounced increase in the oxygen transfer products $(Zr_xO_{2x})^-$ ($x = 1-4$) with higher pressures of CO. Anionic zirconium oxides containing fewer oxygen atoms than the $Zr_xO_{2x+1}^-$ series of clusters were found to weakly adsorb CO while those with more oxygen were shown to lose molecular O_2 through collisional fragmentation, as confirmed by separate experiments with Xe. The ZrO_3^- cluster exhibited the most intense oxygen transfer product accounting for approximately 25% of the total ion intensity at the maximum pressure of 10 mTorr of CO. The $Zr_2O_5^-$, $Zr_3O_7^-$ and $Zr_4O_9^-$ clusters exhibited comparable oxygen transfer products equal to approximately 10% of the total ion intensity at the maximum pressure of 20 mTorr of CO. To facilitate a qualitative comparison of the relative reactivity

Table 1. Experimental Rate Constants (k) Calculated Using the Pseudo-First Order Approximation[a]

Cluster	CO k ($cm^3\ s^{-1}$)	N_2O k ($cm^3\ s^{-1}$)	C_2H_2 k ($cm^3\ s^{-1}$)	C_2H_4 k ($cm^3\ s^{-1}$)
ZrO_3^-	2.1 E−12	4.9 E−12	6.9 E−13	3.1 E−13
$Zr_2O_5^-$	2.2 E−13	2.5 E−12	1.3 E−12	1.4 E−13
$Zr_3O_7^-$	3.4 E−13	1.1 E−12	3.2 E−13	4.5 E−13
$Zr_4O_9^-$	1.8 E−13	7.2 E−13	5.3 E−13	5.4 E−13

[a] The collisional rate constant (k_L) is on the order of 10^{-10} $cm^3\ s^{-1}$. The error bars are estimated to be ± 30%.

of ZrO_3^-, $Zr_2O_5^-$, $Zr_3O_7^-$ and $Zr_4O_9^-$ the phenomenological rate constant at the average laboratory frame energy of 1 eV was calculated for each cluster assuming pseudofirst order kinetics according to eq 2.

$$\ln\left[\frac{I_r}{I_0}\right] = -k[R]t \qquad (2)$$

In eq 2, I_r is the reactant ion intensity with the addition of reactant gas, I_0 is the reactant ion intensity without reactant gas, k is the rate constant, R is the concentration of reactant gas, and t is the time it takes the reactant ion to pass through the octopole reaction cell. The reaction time may be calculated based on the length of the collision cell which was determined using a trapezoidal pressure falloff approximation[33] to be 12.9 cm and the velocity of the ions resulting from the supersonic expansion which was determined using the equations of Anderson and Fenn.[8,50] Therefore, the rate constant takes into account the larger amount of time spent in the reaction cell by heavier clusters due to their lower velocity. Equation 2 assumes that there is not a significant increase in reaction time due to multiple collisions with the neutral reactant gas that slow down the reactant ions in the collision cell. Despite this assumption, previous studies in one of our laboratories have shown that the pseudofirst order rate constants obtained using eq 2 agree well with the phenomenological rate constants calculated from zero pressure cross section data.[8] Assuming pseudofirst order kinetics, the slopes of the plots of $\ln[I_r/I_0]$ vs. reactant gas concentration are equal to $-kt$. The values of the slopes, when divided by reaction time, reveal rate constants on the order of 10^{-13} $cm^3\ s^{-1}$ to low 10^{-12} $cm^3\ s^{-1}$ which are several orders of magnitude below the collisional rate constant (k_L) which is on the order of 10^{-10} $cm^3\ s^{-1}$. The rate constants for each reactant molecule are provided in Table 1. The phenomenological rate constants allow a better qualitative comparison of the relative reactivity of the different clusters than can be obtained from the normalized ion intensities in Figure 1a−d. The kinetic analysis confirms that ZrO_3^- is the most reactive species, followed by $Zr_3O_7^-$, $Zr_2O_5^-$, and last $Zr_4O_9^-$.

Comparison of these experimental results with those for stoichiometric cationic zirconium oxide clusters $(ZrO_2)_x^+$ ($x = 1-4$) reported in a previous publication[6] reveals that the cationic clusters are significantly more reactive than the corresponding anionic species. While the maximum reactant gas pressure in the anion experiments is double that for the cation studies, the intensity of the oxygen transfer products is much lower for the anionic clusters than for the cationic species. Moreover, the rate constants are measured to be roughly one order of magnitude larger for the cationic clusters (10^{-12} $cm^3\ s^{-1}$) than for the anionic clusters (10^{-13} $cm^3\ s^{-1}$). An exception to the overall trend is observed for ZrO_3^- which has a rate constant larger than the other anionic clusters (10^{-12} $cm^3\ s^{-1}$).

The calculated ground-state geometries of ZrO_3^-, $Zr_2O_5^-$, $Zr_3O_7^-$ and $Zr_4O_9^-$, presented in Figure 2a, reveal the common presence of a radical oxygen center in each anionic cluster which is characterized by a longer, weaker bond. The most stable structures with labeled bond lengths as well as the structures of energetically higher lying isomers are provided in the Supporting Information as both a figure and coordinate file. Most of these isomers are higher in energy than the ground-state structures by >1.0 eV and, consequently, do not play any role in the presented reactivity studies. An exception is the $Zr_2O_5^-$ cluster which exhibits a closely lying isomer that is 0.21 eV higher in energy. This isomer is explicitly accounted for in the calculated reaction profiles. The ground-state geometries all have a doublet electronic configuration. The quartet states are all significantly higher in energy. The ground-state geometries of the corresponding stoichiometric cationic clusters, calculated previously,[6] are also provided in Figure 2b for comparison. The structures of neutral zirconium oxide clusters are available in the literature.[51] On the basis of a simplified valence bonding view of metal oxide clusters, anionic species with the stoichiometry $Zr_xO_{2x+1}^-$ (i.e., ZrO_3^-, $Zr_2O_5^-$, $Zr_3O_7^-$ and $Zr_4O_9^-$) contain one more oxygen atom than the neutral stoichiometric $(ZrO_2)_x$ clusters, which, when combined with the additional electron of the anion, generates a single radical oxygen center (M−O•). Therefore, by adding one oxygen atom with a full octet of valence electrons (O^{2-}) to stoichiometric cationic zirconium oxide clusters $(ZrO_2)_x^+$ ($x = 1-4$), a series of anionic clusters is formed containing radical oxygen centers. The structures presented in Figure 2 illustrate that both cationic and anionic metal oxide clusters with specific stoichiometries possess oxygen radical centers with elongated metal−oxygen bonds (elongation ≈ 0.24 ± 0.02 Å). Furthermore, the metal−oxygen bond lengths at the radical centers are comparable between the different charge states. This type of localized oxygen radical center results from the large difference in electron affinity between the zirconium atoms (0.43 eV) and oxygen atoms (1.46 eV) in zirconium oxide clusters. The terminal metal−oxygen bonds in early transition metal oxides can be viewed, approximately, as M═O double bonds. When one electron is missing it results in a localized M−O single bond that is elongated in comparison to the M═O double bond by approximately 0.24 ± 0.02 Å. Moreover, the spin unpaired electron is located on the terminal oxygen atom.

Snapshots from molecular dynamics simulations, presented in Figure 1f for the example cluster $Zr_2O_5^-$, illustrate that the oxidation of CO may occur through the initial binding of CO to the radical oxygen center where the zirconium−oxygen bond is elongated to 2.04 Å from approximately 1.8 Å. The calculated energy profile, displayed in Figure 1e, shows that the initial encounter complex is 1.94 eV more stable than the reactants and contains a bent CO_2 subunit that results from the transfer of charge from the cluster to CO. Subsequent formation of a carbon−zirconium bond involves a barrier that is 0.06 eV higher in energy and results in a complex that is 1.91 eV more stable than the separated reactants. Transfer of charge from CO_2 back to the cluster entails a barrier that is 1.03 eV higher in energy than the initial encounter complex and results in the formation of a structure with a linearly bound CO_2 subunit that is

(50) Anderson, J. B.; Fenn, J. B. *Phys. Fluids* **1965**, *8*, 780.

(51) von Helden, G.; Kirilyuk, A.; van Heijnsbergen, D.; Sartakov, B.; Duncan, M. A.; Meijer, G. *Chem. Phys.* **2000**, *262*, 31–39.

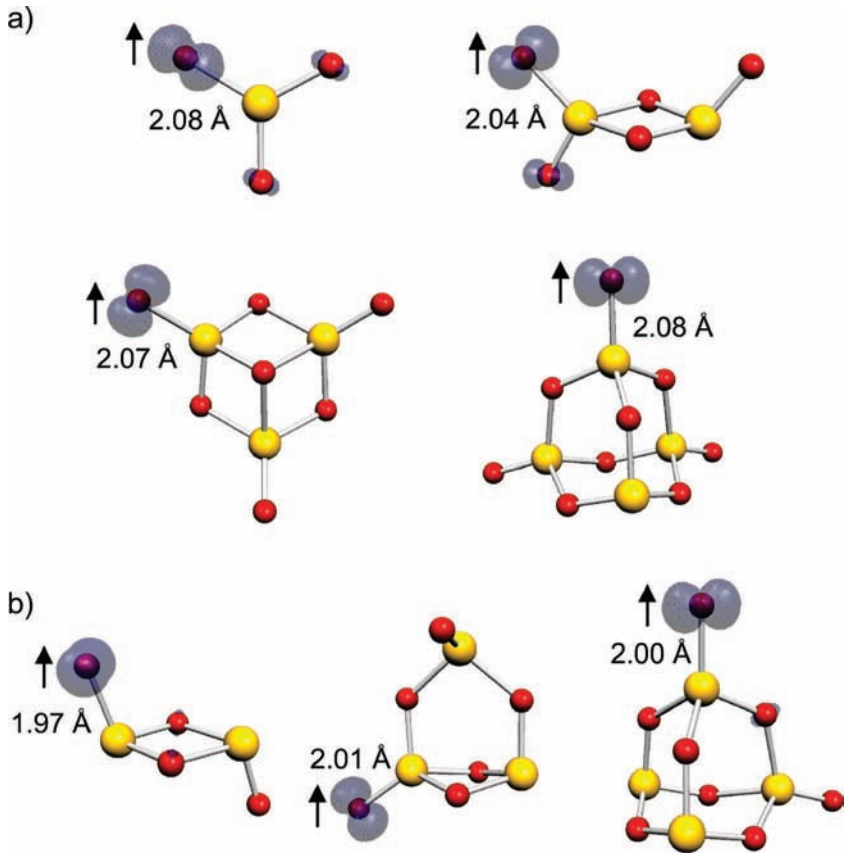

Figure 2. Calculated lowest energy structures for (a) ZrO_3^-, $Zr_2O_5^-$, $Zr_3O_7^-$, and $Zr_4O_9^-$ (b) $Zr_2O_4^+$, $Zr_3O_6^+$, and $Zr_4O_8^+$. The radical oxygen centers are indicated by an arrow. The gray isosurface indicates the localized spin density.

0.98 eV more stable than the reactants. Loss of CO_2 from the cluster requires an additional 0.11 eV of energy and results in the formation of the experimentally observed product $Zr_2O_4^-$. The overall process is calculated to be exothermic by 0.87 eV and to involve a barrier that is lower in energy than that of the separated reactants. The oxidation of CO by ZrO_3^-, $Zr_3O_7^-$ and $Zr_4O_9^-$ proceeds according to this general mechanism due to the common presence of the same oxygen radical center in each of the anionic $Zr_xO_{2x+1}^-$ ($x = 1-4$) clusters.

Comparison of the energy profile presented in Figure 1e with the profile calculated previously[6] for the corresponding cationic cluster containing an oxygen radical center ($Zr_2O_4^+$) reveals that the mechanisms are very similar between different charge states, but that the overall process is more exothermic in the cationic case (1.65 eV for cation vs. 0.87 eV for anion). Formation of the initial encounter complex is exothermic by 1.94 eV for anionic $Zr_2O_5^-$, while for cationic $Zr_2O_4^+$ 1.60 eV is gained through complex formation. Furthermore, the barrier to the rearrangement involving transfer of charge from CO_2 back to the cluster is larger (1.03 eV) for the anionic cluster than for the cationic species (0.29 eV).[6] This is because the electron is more attracted to the cationic cluster than to the anionic species. Therefore, although oxygen radical centers in both cationic and anionic metal oxide clusters promote the oxidation of CO, charge state directly influences the energy barrier in the critical step leading to CO_2 formation.

In a recent publication[6] we showed that stoichiometric cationic zirconium oxide clusters containing radical oxygen centers $(ZrO_2)_x^+$ ($x = 1-4$) may be regenerated from oxygen deficient clusters using a strong oxidant. To determine whether regeneration of radical oxygen centers in anionic clusters is also possible we reacted stoichiometric anionic zirconium oxide clusters $(ZrO_2)_x^-$ ($x = 1-4$) with N_2O. Each cluster was found to strongly add only one oxygen atom, consistent with the formation of the radical oxygen containing anionic stoichiometry according to eq 3.

$$(ZrO_2)_x^- (x = 1-4) + N_2O \rightarrow Zr_xO_{2x+1}^- + N_2 \qquad (3)$$

The normalized ion intensities of ZrO_2^-, $Zr_2O_4^-$, $Zr_3O_6^-$ and $Zr_4O_8^-$ with increasing pressure of N_2O are provided in the Supporting Information. With increasing pressure of N_2O the intensity of the stoichiometric clusters $(ZrO_2)_x^-$ ($x = 1-4$) decreases while that of the oxygen addition products $(Zr_xO_{2x+1})^-$ ($x = 1-4$) becomes more pronounced. ZrO_2^- exhibited the most intense oxygen addition product corresponding to approximately 50% of the total ion intensity at the maximum N_2O pressure of 10 mTorr. Using the pseudofirst order kinetics method described above for CO, the phenomenological rate constants were calculated for the oxidation of each stoichiometric cluster to the active $Zr_xO_{2x+1}^-$ species. The rate constants were determined to be on the order of high 10^{-13} cm^3 s^{-1} to mid 10^{-12} cm^3 s^{-1}. Therefore, the rate constants for the regeneration of the anionic oxygen radical centers, provided in Table 1, are larger than the rate constants for the oxidation of CO by a factor of roughly 2, 11, 3, and 4 for ZrO_3^-, $Zr_2O_5^-$, $Zr_3O_7^-$, and $Zr_4O_9^-$, respectively.

Snapshots from molecular dynamics simulations of the oxidation of the example cluster, $Zr_2O_4^-$, by N_2O are shown in Figure 3, indicating the regeneration of the active oxygen radical center. Both experiment and theory, therefore, suggest that anionic metal oxide clusters containing oxygen radical centers may promote a full catalytic cycle for the oxidation of CO.

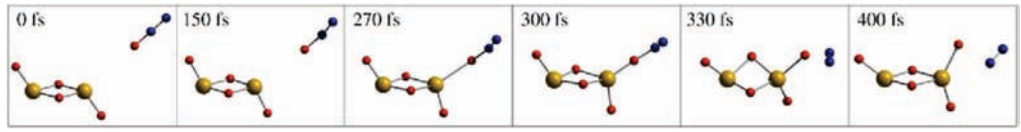

Figure 3. Snapshots from MD simulations of the reaction of $Zr_2O_4^-$ with N_2O.

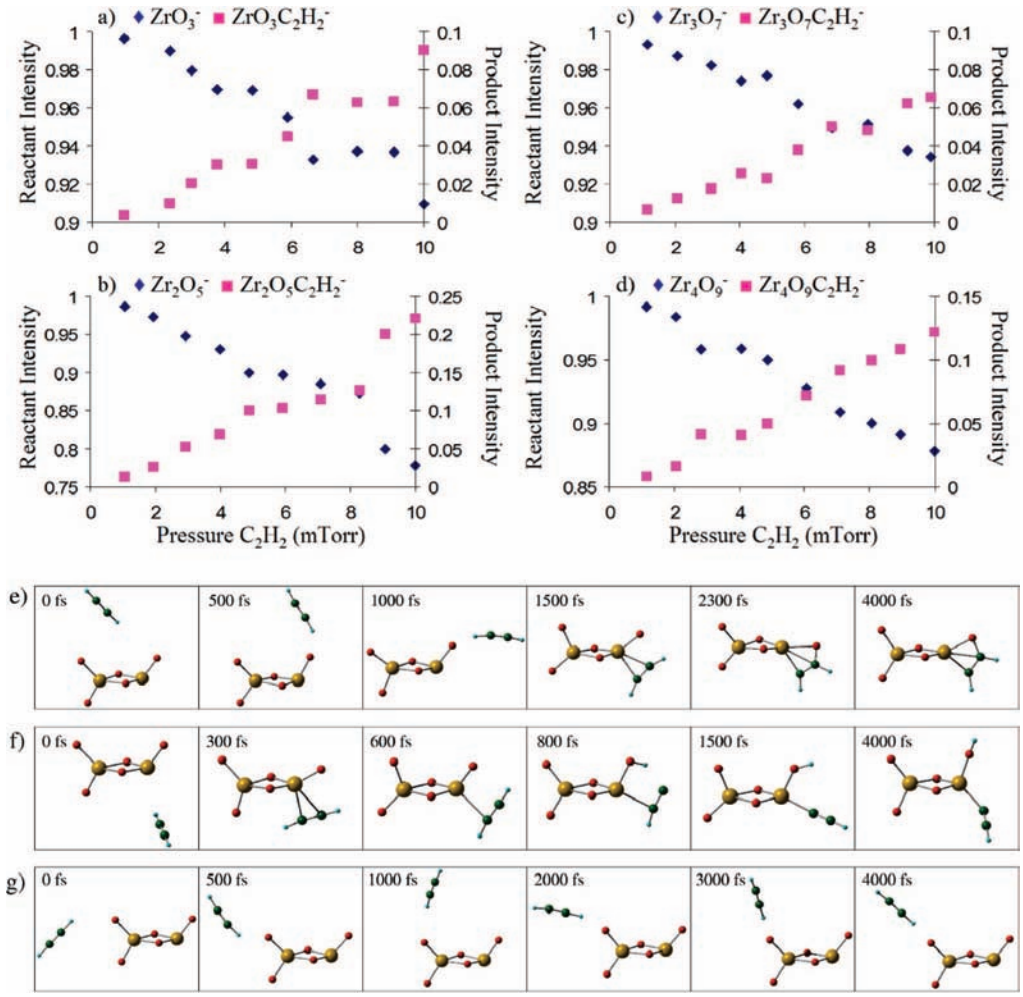

Figure 4. Normalized ion intensities of (a) ZrO_3^- (b) $Zr_2O_5^-$ (c) $Zr_3O_7^-$ and (d) $Zr_4O_9^-$ with increasing pressure of C_2H_2. (e−g) Snapshots from MD simulations of the reaction of $Zr_2O_5^-$ with C_2H_2.

When reacted with C_2H_2 the $Zr_xO_{2x+1}^-$ ($x = 1-4$) series of anionic clusters exhibited association products consistent with eq 4.

$$Zr_xO_{2x+1}^- (x = 1-4) + C_2H_2 \rightarrow Zr_xO_{2x+1}C_2H_2^- \qquad (4)$$

The normalized ion intensities of ZrO_3^-, $Zr_2O_5^-$, $Zr_3O_7^-$ and $Zr_4O_9^-$ with increasing pressures of C_2H_2 are presented in Figure 4a−d. $Zr_2O_5^-$ has the most intense C_2H_2 association product followed by $Zr_4O_9^-$, ZrO_3^- and finally, $Zr_3O_7^-$. Using the pseudofirst order kinetics method described above for CO, the phenomenological rate constants for the association of C_2H_2 were determined to be on order of 10^{-13} cm^3 s^{-1} to low 10^{-12} cm^3 s^{-1}, as shown in Table 1.

These C_2H_2 association products are in stark contrast to the oxidation observed previously for stoichiometric cationic zirconium oxides containing radical oxygen centers.[6] The cationic $(ZrO_2)_x^+$ ($x = 1-4$) clusters all exhibited strong oxygen transfer products when reacted with C_2H_2. Only minor association of C_2H_2 was observed onto the $Zr_3O_6^+$ and $Zr_4O_8^+$ clusters.

Snapshots from molecular dynamics simulations, displayed in Figure 4e−g for the example cluster $Zr_2O_5^-$, reveal that C_2H_2 associates in two possible configurations: at the less coordinated zirconium atom and at the oxygen radical center (compare Figure 4e−g). The more strongly bound arrangement results from C_2H_2 binding to the less coordinated zirconium atom as shown in Figure 4e. The corresponding calculated energy profile, presented in Figure 5, reveals that the initial encounter complex that forms is 2.05 eV more stable than the separated reactants. In the initial encounter complex, the spin density of the oxygen radical is localized on one of the oxygen atoms on the opposite side of the cluster to where C_2H_2 associates. Therefore, significant structural rearrangement must occur to enable interaction between an oxygen atom with radical character and C_2H_2. Breaking of the zirconium−carbon bonds and migration of a peripheral oxygen atom to a bridging position between the two zirconium atoms involves a barrier that is 1.07 eV high in energy. This process results in the formation of a structure containing an oxidized acetylene molecule with the spin density

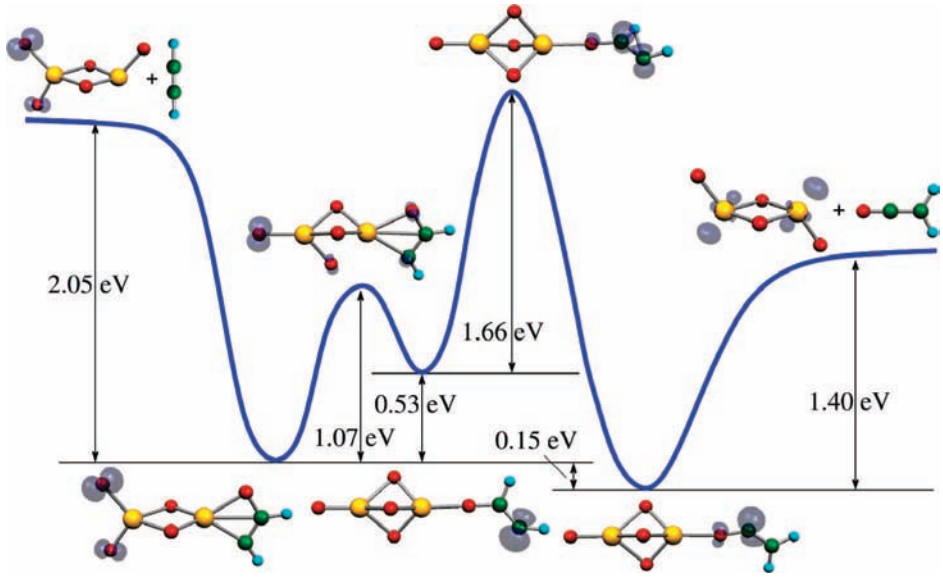

Figure 5. Calculated energy profile for the reaction of $Zr_2O_5^-$ with C_2H_2. The gray isosurface indicates the localized spin density.

localized on one carbon atom of the C_2H_2O subunit. This intermediate is higher in energy by 0.53 eV than the initial encounter complex. Subsequent hydrogen transfer, which is critical to enable oxidation, is unfavorable due to a large barrier of 1.66 eV. The anionic ZrO_3^-, $Zr_3O_7^-$ and $Zr_4O_9^-$ clusters also associate C_2H_2 and are unreactive toward oxidation due to the common presence of a large barrier to the critical hydrogen transfer step that is higher in energy than the reactants.

The energy profile for the oxidation of C_2H_2 by cationic zirconium oxide clusters containing oxygen radical centers, calculated previously,[6] reveals a very different situation. Formation of the initial encounter complex between C_2H_2 and $Zr_2O_5^-$ is less exothermic (2.05 eV) than for the corresponding cationic $Zr_2O_4^+$ cluster which gains 2.63 eV from association of C_2H_2.[6] For the cationic cluster, C_2H_2 binds directly to the oxygen radical center and the adjacent zirconium atom, while for the anionic species, C_2H_2 associates preferentially to the less coordinated zirconium atom which is on the opposite side of the cluster to the oxygen radical center. Consequently, the mechanism leading to the oxidation of C_2H_2 requires significant structural rearrangement. This results in a hydrogen transfer step that, while favorable for the cationic clusters, involves a much higher barrier for the anionic species as shown in Figure 5. Moreover, the overall process is calculated to be far more exothermic (1.57 eV) for the cationic cluster than for the anionic species (0.80 eV).

In addition to the mechanism described above, we theoretically investigated an alternative reaction pathway for the oxidation of C_2H_2 assuming initial association to the less coordinated zirconium atom of $Zr_2O_5^-$. This mechanism involves direct loss of HCCHO from the cluster prior to a considered hydrogen transfer. The estimated barrier of around 0.3 eV with respect to the reactants makes the oxidation process along this reaction pathway also unfavorable for the $Zr_2O_5^-$ species.

Although MD simulations revealed that C_2H_2 associates preferentially to the less coordinated zirconium atom which is on the opposite side of the anionic cluster to the radical oxygen, we also calculated the energy profiles for the oxidation of C_2H_2 at the radical oxygen center to identify the barriers preventing reaction at this site. The energy profiles are provided in the Supporting Information. Briefly, formation of a bond between a carbon atom of C_2H_2 and the radical oxygen is calculated to involve a barrier of 0.11 eV. If this barrier were to be surmounted, the initial encounter complex that forms would consist of C_2H_2 bound in a ring configuration to the radical oxygen and the adjacent oxygen and zirconium atoms and is lower in energy than the reactants by 3.17 eV. From the initial encounter complex, three oxidation mechanisms, all of which require a hydrogen transfer step involving a large energy barrier were identified. Due to these barriers the oxidation of C_2H_2 is unfeasible and is not observed experimentally or in the MD simulations.

The second, more weakly bound configuration identified by the MD simulations involves the association of C_2H_2 onto the oxygen radical center of the cluster as shown in Figure 4g. This linear arrangement, which is 0.29 eV more stable than the separated reactants, is similar to the initial encounter complex observed between CH_4 and a radical oxygen in $Al_8O_{12}^+$ by Feyel and co-workers.[52] To investigate whether hydrogen atom abstraction from C_2H_2 may occur at radical oxygen centers in anionic clusters, the energy barrier to the formation of a hydroxy group was calculated and is estimated to be at least 1 eV. Therefore, hydrogen abstraction from unsaturated hydrocarbons is not favorable at oxygen radical centers in anionic zirconium oxide clusters. However, snapshots from molecular dynamics simulations, displayed in Figure 4f, reveal that hydrogen abstraction may occur when C_2H_2 associates to the less coordinated zirconium atom of the cluster. In this more strongly bound configuration (binding energy = 0.85 eV) the calculated barrier to hydrogen abstraction is 0.47 eV lower in energy than the reactants. Unfortunately, due to the isotope distribution of zirconium and no mass change in the process, we were unable to experimentally identify the process of hydrogen abstraction from C_2H_2 by anionic zirconium oxide clusters.

The $Zr_xO_{2x+1}^-$ ($x = 1-4$) series of anionic clusters were found experimentally to exhibit minor products consistent with the association of C_2H_4 according to eq 5.

(52) Feyel, S.; Döbler, J; Hockerdorf, R.; Beyer, M. K.; Sauer, J.; Schwarz, H. *Angew. Chem., Int. Ed.* **2008**, *47*, 1946–1950.

$$Zr_xO_{2x+1}^- (x = 1-4) + C_2H_4 \rightarrow Zr_xO_{2x+1}C_2H_4^- \quad (5)$$

Low intensity association products were observed with increasing pressures of C_2H_4 as shown in the experimental branching ratios provided in the Supporting Information. To enable a qualitative comparison of the relative C_2H_4 association reactivity of the $Zr_xO_{2x+1}^-$ ($x = 1-4$) clusters, the phenomenological rate constants were calculated as described above for CO. The rate constants were determined to be on the order of 10^{-13} cm^3 s^{-1}.

Snapshots from molecular dynamics simulations, presented in Figure 6b for the example cluster, $Zr_2O_5^-$, reveal that ethylene, like acetylene, associates preferentially to the less coordinated zirconium atom. The initial encounter complex is calculated to be 1.03 eV lower in energy than the reactants as shown in the energy profile in Figure 6a. In the initial encounter complex, the spin density of the oxygen radical is localized on one of the oxygen atoms on the opposite side of the cluster to where C_2H_4 associates. Therefore, as was the case with C_2H_2, significant structural rearrangement is necessary to enable the interaction of C_2H_4 with an oxygen atom having radical character. Dissociation of the zirconium−carbon bond and migration of a peripheral oxygen atom to a bridging configuration between the two zirconium atoms involves a transition state that is 1.07 eV higher in energy and results in an intermediate containing an oxidized ethylene molecule with the spin density localized on one carbon atom of the C_2H_4O subunit. This arrangement is almost equal in energy to the initial encounter complex. Subsequent transfer of hydrogen from the carbon atom bound to oxygen to the other carbon atom of ethylene involves a barrier that is 1.57 eV higher in energy. Furthermore, the overall process for the formation of acetaldehyde is calculated to be exothermic by only 0.03 eV. ZrO_3^-, $Zr_3O_7^-$ and $Zr_4O_9^-$ are observed to weakly associate C_2H_4 due to the common presence of a large barrier to the necessary structural rearrangement and hydrogen transfer step leading to formation of acetaldehyde.

Comparison of the energy profile presented in Figure 6a with the one calculated previously[6] for $Zr_2O_4^+$ reveals major differences between charge states. Formation of the initial encounter complex is far more exothermic for the cationic cluster (1.90 eV) than for the anionic species (1.03 eV). Ethylene binds directly to the oxygen radical of the cationic cluster but associates preferentially to the less coordinated zirconium atom of the anionic species which is on the opposite side of the cluster to the oxygen radical. Therefore, the hydrogen transfer step involves a larger barrier (1.57 eV) for $Zr_2O_5^-$ than for $Zr_2O_4^+$ (1.11 eV). Additionally, the overall process leading to formation of acetaldehyde, is exothermic for the cationic cluster by 0.80 eV, but only by 0.03 eV for the anionic species. Consequently, due to the more weakly bound nature of the initial encounter complex, insufficient energy is available to promote the structural rearrangement that would allow C_2H_4 to interact with the active site in the anionic cluster.

Although the MD simulations revealed that C_2H_4 binds preferentially to the less coordinated zirconium atom of anionic $Zr_2O_5^-$, we nevertheless calculated the energy profile for the oxidation of C_2H_4 at the radical oxygen center to determine if similar barriers to those calculated for C_2H_2 are also present for C_2H_4. The energy profile is provided in the Supporting Information for the interested reader. Briefly, binding of C_2H_4 directly to the oxygen radical of anionic $Zr_2O_5^-$ is calculated to involve a barrier of 0.10 eV. If this barrier were to be overcome, the initial encounter complex that forms is calculated to be 1.98 eV more stable than the separated reactants. However, the subsequent barrier to the critical hydrogen transfer step necessary for the formation of acetaldehyde is calculated to be 0.51 eV higher in energy than the reactants. Oxidation of C_2H_4 at anionic zirconium oxide clusters containing radical oxygen centers, therefore, is kinetically unfavorable and is not observed either in the experiments or the MD simulations.

The qualitative explanation for the different reactivity of cationic and anionic zirconium oxide clusters, in spite of the common presence of the oxygen radical center for specific stoichiometries, can be understood from the calculated maps of the molecular electrostatic potential (MEP). As can be seen in Figure 7a for the case of the example cluster, $Zr_2O_5^-$, the MEP exhibits largely negative values at the molecular surface and is only positive close to the less coordinated zirconium atom. This indicates that nucleophilic molecules such as C_2H_2 and C_2H_4 will bind to the less coordinated zirconium atom with positive values of MEP as confirmed by the MD simulations (cf. Figures 4e and 6b). CO, in contrast to C_2H_2 and C_2H_4, has a dipole moment (0.112 D) and can bind both to the radical center as well as to the less coordinated zirconium atom of the anionic cluster. In comparison to anionic $Zr_2O_5^-$, the MEP of cationic $Zr_2O_4^+$, shown in Figure 7b, is positive over the entire cluster surface and, therefore, nucleophilic molecules will bind both to the zirconium as well as to the oxygen atoms. In the latter case, attack at the oxygen radical center leads to the oxidation reactions since the subsequent barriers to the hydrogen transfer steps are easily surmountable as shown previously.[6] This indicates that an interplay between the relative electrostatic potential and hydrogen transfer barriers causes the different reactivity observed for anionic versus cationic zirconium oxide clusters. Therefore, in the case of cationic stoichiometric clusters $(ZrO_2)_x^+$ ($x = 1-4$) the oxidation reaction proceeds for CO, C_2H_2 and C_2H_4, and in the case of anionic clusters $(Zr_xO_{2x+1})^-$ ($x = 1-4$) the oxidation reaction proceeds only for CO.

Conclusions and Outlook

Through a combination of gas-phase experiments and density functional theory calculations we provide evidence that charge state directly influences whether the oxidation of unsaturated hydrocarbons is favorable at metal oxide clusters containing radical oxygen centers. By adding one oxygen atom with a full octet of valence electrons (O^{2-}) to stoichiometric cationic zirconium oxide clusters $(ZrO_2)_x^+$ ($x = 1-4$), a series of anionic clusters are formed containing radical oxygen centers with elongated (elongation $\approx 0.24 \pm 0.02$ Å) zirconium−oxygen bonds. The anionic clusters are shown to oxidize CO, strongly associate C_2H_2, and weakly associate C_2H_4. Calculations indicate that the oxidation of CO is favorable and involves easily surmountable energy barriers. The oxidation of C_2H_2 and C_2H_4, however, requiring a critical hydrogen transfer step, is calculated to be energetically unfavorable at anionic zirconium oxide clusters containing radical oxygen centers. These results are in contrast to our previous findings for cationic stoichiometric zirconium oxides where all three molecules were shown to be easily oxidized. The influence of charge state on reactivity may be qualitatively understood from the relative difference in the calculated electrostatic potential of the clusters. Nucleophilic reactants will interact favorably with the entire surface of the cationic clusters. The anionic clusters, in contrast, bind nucleophiles preferentially to the less coordinated zirconium atom where the values of the molecular electrostatic potential are

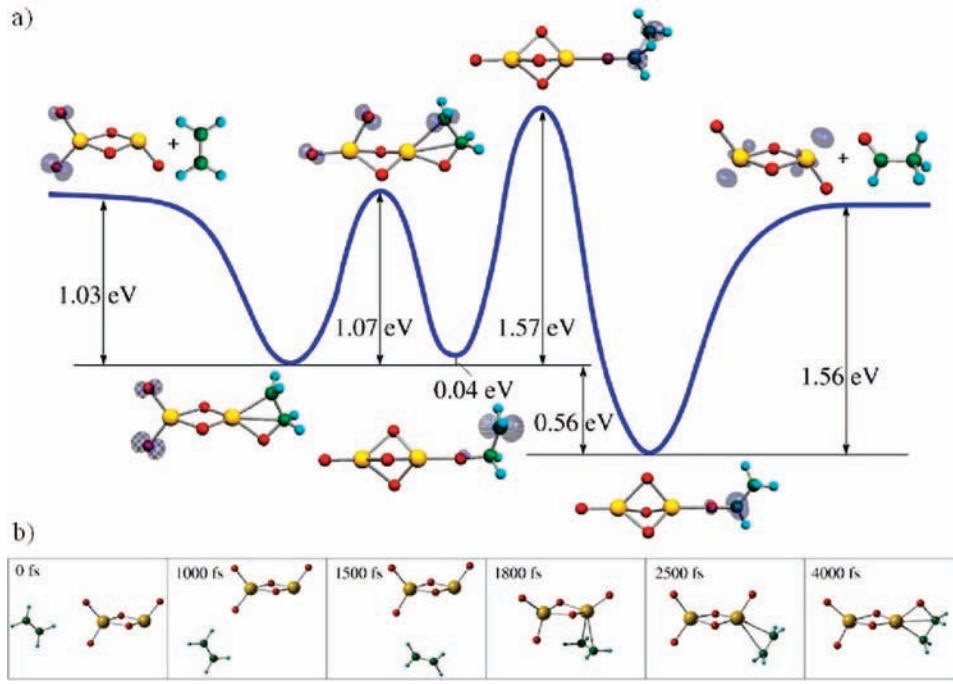

Figure 6. (a) Calculated energy profile for the reaction of $Zr_2O_5^-$ with C_2H_4. The gray isosurface indicates the localized spin density. (b) Snapshots from MD simulations of the reaction of $Zr_2O_5^-$ with C_2H_4.

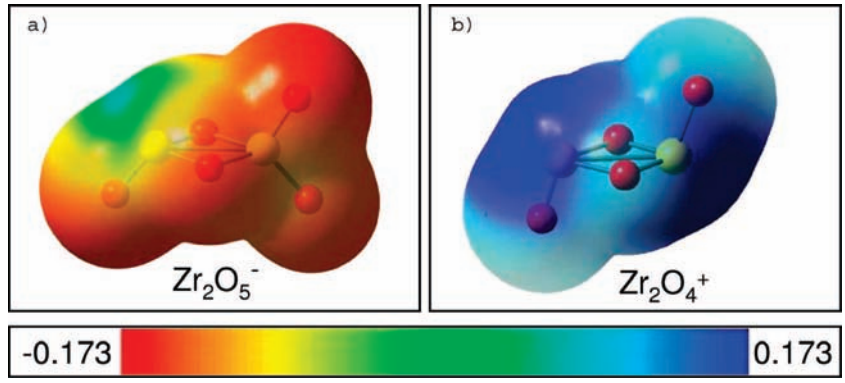

Figure 7. Calculated molecular electrostatic potential (MEP) for the (a) anionic and (b) cationic example of zirconium oxide clusters with radical oxygen centers projected onto the constant electron density surface with iso value 0.0004. The color scales from red over green to blue labeling transitions from negative to positive values illustrating the different ability of anionic and cationic charge states to react with nucleophilic or electron rich molecules.

positive. Finally, anionic clusters containing radical oxygen centers may be regenerated by reacting oxygen deficient clusters with a strong oxidizer. Therefore both anionic and cationic metal oxide clusters containing radical oxygen centers may exhibit a full catalytic cycle for the oxidation of CO. However, the oxidation of C_2H_2 and C_2H_4 is most efficient in the presence of clusters with a combination of a radical oxygen center and positive charge. Comparison of the rate constants for the oxidation of C_2H_4 by $Zr_2O_4^+$ and $Zr_4O_8^+$ (low 10^{-12} cm^3 s^{-1}) and $V_2O_5^+$ and $V_4O_{10}^+$ (high 10^{-10} cm^3 s^{-1})[8] suggests that higher overall reaction efficiency may be attainable with oxide clusters of 3d rather than 4d transition metals. Nevertheless, zirconium oxide clusters serve as a useful model system to investigate the catalytic activity of radical oxygen centers that are known to exist in bulk-phase metal oxides.

Our findings concerning the influence of charge state on catalytic oxidation reactions at zirconium oxide clusters containing radical oxygen centers have conceptual ramifications for the design of future heterogeneous oxidation catalysts. As mentioned previously, radical oxygen centers have been suggested to be responsible for the selective oxidation of a variety of industrially relevant molecules over bulk-phase V_2O_5 and MoO_3 catalysts.[16] Indeed, radical centers in MoO_3/SiO_2 and V_2O_5/SiO_2 catalysts have been suggested to be responsible for the selective oxidation of methane to methanol and formaldehyde,[13] the oxidative dehydrogenation of ethane,[14] and the hydroxylation of benzene to phenol.[15] Radical oxygen centers have also been identified in neutral gas-phase clusters such as VO_3.[53] Therefore, through a controlled deposition of size selected clusters onto chosen supports,[54−56] it may be possible

(53) Dong, F.; Heinbuch, S.; Xie, Y.; Rocca, J. J.; Bernstein, E. R.; Wang, Z. C.; Deng, K.; He, S. G. *J. Am. Chem. Soc.* **2008**, *130*, 1932–1943.
(54) Abbet, S.; Judai, K.; Klinger, L.; Heiz, U. *Pure Appl. Chem.* **2002**, *74*, 1527–1535.
(55) Perez, A.; Melinon, P.; Dupuis, V.; Jensen, P.; Prevel, B.; Tuaillon, J.; Bardotti, L.; Martet, C.; Treilleux, M.; Broyer, M.; Pellarin, M.; Vaille, J. L.; Palpant, B.; Lerme, J. *J. Phys. D: Appl. Phys.* **1997**, *30*, 709–721.

to create catalyst materials with a high concentration of oxygen radical centers that would promote industrially relevant oxidation reactions. Alternatively, it has been shown that by doping metal oxides such as MgO with an element like Li that has one less valence electron, it is possible to generate radical oxygen centers in bulk metal oxides.[57,58] Based on these previous findings, we propose that by doping neutral stoichiometric zirconium oxide clusters $(ZrO_2)_x$ with a metal containing one less valence electron (i.e., Y or Sc) it may be possible to generate neutral metal oxide clusters with localized radical oxygen centers. These clusters should have catalytic properties closely resembling the cationic stoichiometric zirconium oxide clusters discussed in our previous publication.[6] Therefore, they would be expected to serve as active sites for the selective oxidation of CO to CO_2, C_2H_4 to acetaldehyde, and C_2H_2 to ethenone. Furthermore, by doping neutral stoichiometric zirconium oxide clusters with a metal containing one additional valence electron (i.e Nb or V), and exposing them to a strong oxidizer such as N_2O, it would be possible to generate neutral zirconium oxide clusters with a $Zr_{x-1}NbO_{2x+1}$ stoichiometry. The one additional oxygen atom and electron from the dopant atom should form an oxygen radical center that would be expected to exhibit reactivity similar to the anionic zirconium oxide clusters discussed herein. Therefore, p-type doping of zirconium oxides is expected to result in the formation of clusters that promote the oxidation of CO, C_2H_4 and C_2H_2, while n-type doping would create clusters that only promote the oxidation of CO.

Acknowledgment. G.E.J., E.C.T. and A.W.C. gratefully acknowledge the Department of Energy, Grant Number DE-FG02-92ER14258, for their financial support. R.M., M.N. and V.B.K. acknowledge the Deutsche Forschungsgemeinschaft. A.W.C. also acknowledges the Humboldt Foundation for a US Senior Scientist Award during which time much of this paper was prepared at the institute of Professor V. Bonačić-Koutecký, Humboldt University, Berlin. The hospitality of the institute is also gratefully acknowledged.

Supporting Information Available: Calculated ground-state structures and energetically higher lying isomers of anionic zirconium oxide clusters and energy profiles for the reaction of $Zr_2O_5^-$ with carbon monoxide, acetylene and ethylene using the B3LYP and PBE functionals are provided. Experimental ion intensity ratios for reactions with N_2O and C_2H_4 are also supplied. This material is available free of charge via the Internet at http://pubs.acs.org.

JA807499Z

(56) Trainoff, D.; Bardotti, L.; Tournus, F.; Guiraud, G.; Boisron, O.; Melinon, P. *J. Phys. Chem. C* **2008**, *112*, 6842–6849.
(57) Pacchioni, G. *J. Chem. Phys.* **2008**, *128*, 1–10.
(58) Tohver, H. T.; Henderson, B.; Chen, Y.; Abraham, M. M. *Phys. Rev. B.* **1972**, *5*, 3276–3284.